The effects of downstream magnetic field on current-free double layers and beam formation in the Njord helicon plasma device

2010 Plasma Sources Sci. Technol. 19 034009

(http://iopscience.iop.org/0963-0252/19/3/034009)

Plasma Sources Sci. Technol. **19** (2010) 034009 (5pp) doi:10.1088/0963-0252/19/3/034009

The effects of downstream magnetic field on current-free double layers and beam formation in the Njord helicon plasma device

Å Fredriksen, L N Mishra and H S Byhring

Department of Physics and Technology, University of Tromsø, 9037 Tromsø, Norway

E-mail: ashild.fredriksen@uit.no

Received 3 August 2009, in final form 5 November 2009
Published 21 May 2010
Online at stacks.iop.org/PSST/19/034009

Abstract

The Njord device was constructed with the aim of investigating instabilities and turbulence in plasmas with flows and beams, which are common also in space plasmas. Njord is an inductively coupled helicon plasma device with 13.56 MHz RF power inserted into the working gas by means of a saddle antenna through a 13.8 cm inner diameter Pyrex tube. The source plasma expands through a 7 cm long and 20 cm wide port into a 0.6 m diameter and 1.2 m long chamber. Two magnetic field coils around the source and one additional downstream coil produce a magnetic field of about 25 mT at maximum.

We have characterized current-free double layers in argon plasmas, and we find that they are generated at the position where the plasma expands into the main chamber. Further, the effect of shaping the magnetic field from an expanding one to a mirror shaped field by means of the downstream coil has been investigated. The downstream density and the plasma potential increase significantly when all the magnetic field lines in the source are passing also through the port–dome intersection without intersecting the port walls. The ion beam disappears when the plasma potential increases up to a potential similar to that in the source.

(Some figures in this article are in colour only in the electronic version)

1. Introduction

Plasmas expanding along magnetic field lines are common in space. Some of the most obvious examples can be found in the polar cusp region of the Earth and in the solar corona.

In the solar corona, the coronal field contains up- and down-flowing plasma in open as well as closed loops on all scales, leading to red- and blue-shifts of coronal ultraviolet emission lines, and in particular to sporadic blue-shifts within the open field lines (funnels) [1]. The polar wind expels H^+, He^+, O^+ ions into the magnetosphere, and electrons into the ionosphere. It undergoes transitions from subsonic to supersonic flow and from collision-dominated to collisionless regimes [2]. Observations in the ionosphere and magnetosphere have shown that plasma is not only flowing due to the expanding magnetic field lines; double layers (DLs) set up electric fields parallel to the magnetic field in the polar cavity and accelerate the plasma ions and electrons to supersonic speeds and beams [3–5]. Over the years, DLs have been studied in great detail both theoretically and experimentally, as described in several reviews [6–8] and more specific works [9–15].

Although extensive double-layer studies have been performed since the 1970s, only more recently were self-consistent, current-free double layers (CFDLs) in laboratory experiments reported [16–18]. A CFDL is understood as a potential structure where the ion background drift v_d is much less than the thermal electron speed $v_{e,th}$ or $\sim$0, that is without a requirement of a relative electron–ion drift to form the DL, while previously, most laboratory DLs would require a plasma current [16]. The evidence that DLs form at the expansion of plasma into a plasma chamber from a high-density source has over the recent years inspired a large body of experiments on CFDLs.

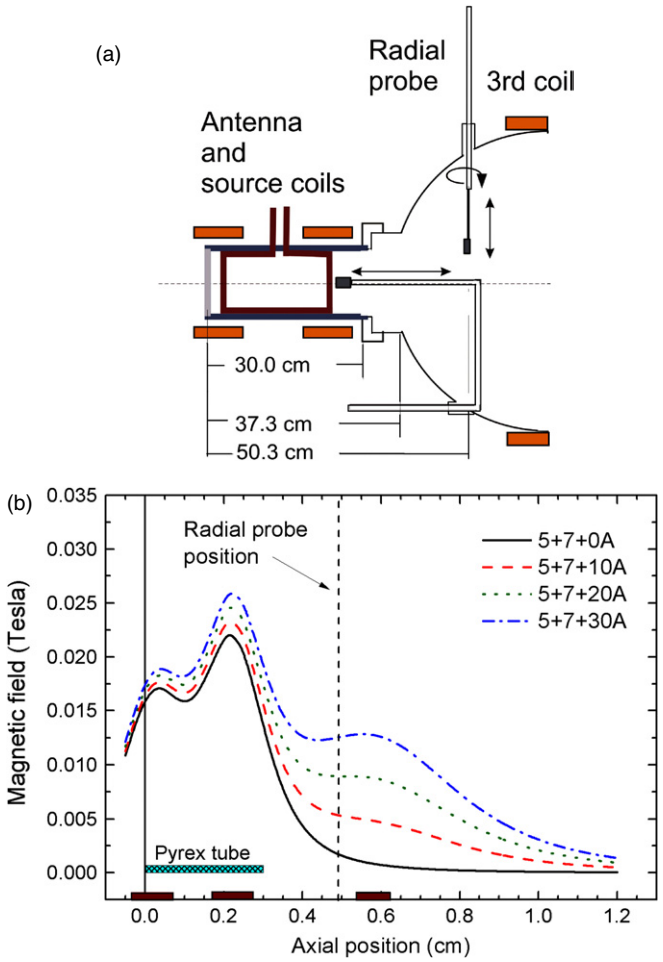

Figure 1. RF source with probe positioning (*a*) and axial magnetic field for four different currents in the third coil (*b*). Positions of the source glass tube and the coils are indicated on the z-axis.

The CFDL accelerates ions from the source into a beam with a beam energy of the order of the difference between the plasma potential (V_p) in the source and in the chamber, and this property has prompted initiatives to develop these sources into plasma propulsion systems for satellites. The study of plasmas and instabilities with flows and ion beams is one of the main objectives behind the construction of the device presented in this paper. The flow of plasma from a source along expanding magnetic field lines bears a strong similarity to many space plasmas, including the ones described above. In section 2 we describe the experiment and diagnostics used to study the beam and flow formation and how it is affected by the shaping of the downstream magnetic field. The results are discussed in section 3.

2. The Experiment

The Njord device consists of a 0.6 m diameter and 1.5 m long chamber with a spherical dome at one end, as shown in figure 1. It has four 35 mm inner diameter (ID) ports and a 200 mm ID flange at the dome end. The chamber is pumped down by a Leybold 600 turbo pump in combination with a rotary pump to a base pressure of typically 0.05–0.1 mPa. A helicon plasma source built at the Australian National University (ANU) after the same specifications as the source of the Chi Kung device at ANU [19] is attached to the 200 mm port, as shown in figure 1. The source is constructed from a 30 cm long Pyrex glass tube with an ID of 13.8 cm. The outer edge of the tube is chosen as the origin of the z-axis for measurements along the centre of the column. A Boswell-type saddle antenna is formed around the tube and maintained at a distance of about 5–10 mm from the glass by means of insulating spacers. The tube and antenna are enclosed by a cylindrical aluminium former holding a pair of magnetic field coils with a diameter of 24 cm and a width of 9.5 cm. The centre of the first coil is placed 18 mm downstream of the outer edge of the Pyrex tube, and the centre of the second is displaced by 20 cm with respect to the centre of the first. A 6 A current in both coils produces maxima of the magnetic fields of about 25 mT. A 68 cm diameter, third coil (guide coil) is placed 58 cm downstream from the origin, close to the intersection between the dome and the main chamber. It produces about 8 mT at 20 A current. 13.56 MHz RF power, typically 300–800 W forward and less than 50 W reflected, is fed from a Henry 8K Ultra amplifier to the antenna through an air-cooled π-matching network consisting of two variable vacuum capacitors. Three radially and one axially oriented ports of the dome are placed 50 cm downstream from the origin at the outer edge of the Pyrex tube, as shown in figure 1. Probes can be inserted through these ports, providing measurements along the axial and radial directions.

For the data presented here, retarding field energy analyzers (RFEAs) were used to obtain plasma potential, and beam density and energy. The RFEA placed in the radial port (figure 1(*a*)) could be rotated 360° around its own axis. The RFEA on the axial through feed faced the source. The grids and plates of the RFEAs [20] were organized 0.5 mm apart as follows: an aperture plate with a gridded 2 mm diameter hole, an electron repeller grid biased at typically −90 V, a discriminator grid swept from −100 to +100 V at zero offset, a secondary electron repeller grid biased at −18 V and a collector plate at −9 V with respect to ground. To capture the energy distribution at the plasma potential, additional batteries between the sweep output and the grid produced positive offsets up to 90 V in steps of 9 V. The discriminator was biased in 400 steps per sweep. At each step, the collector current, measured over a 10 kΩ resistor, was digitized into 300 samples which were then averaged into a single value, and added to the file for further processing.

In the experiments reported here, the following settings were used for the parameters: RF power 400–600 W, argon gas fill pressure from 0.013 to 0.02 Pa (1.2–1.5 sccm). The currents in the first and second source coils were set to 5 A and 7 A, respectively, where the first is at the outer end of the source. The current in the third coil was varied between 0 and 30 A. Some resulting B fields are shown in figure 1(*b*).

3. Results and discussion

It has been reported earlier [21] that in the Njord device, CFDLs form at pressures between 0.0133 and 0.057 Pa, and at second source coil currents larger than 3 A ($\gtrsim$11 mT at second

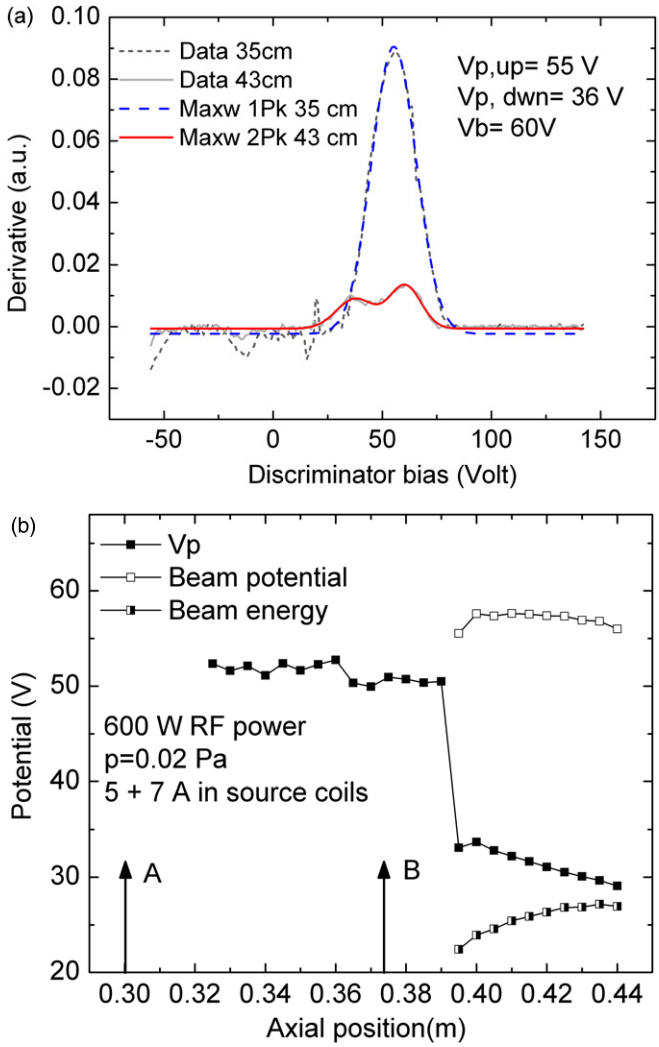

Figure 2. Typical IEDFs from the derivative of RFEA current versus bias traces from one upstream at $z = 30.5$ cm and one downstream position (43 cm), respectively (a), and plasma and beam potentials versus axial position in steps of 0.5 cm (b). The arrow labelled 'A' indicates the end position of the Pyrex tube at $z = 30.5$ cm, and the 'B' arrow indicates the position of the port–dome intersection. Resulting beam energy is shown as half-filled squares.

maximum). DL beams were also observed at downstream radial positions up to 11 cm. We will report here on data taken at typically 0.02 Pa (1.5 sccm flow rate) and with 5 A and 7 A in the first and second source coils, respectively, while the third coil current was varied between 0 and 30 A. RF power was set at 400 or 600 W. To obtain the ion energy distribution functions (IEDF), the current versus bias trace (I–V curve) from the RFEA collector was differentiated with respect to voltage and Gaussian functions were fitted to the resulting experimental distributions, by means of a 'multi-peak' fitting routine in the Origin™ software. In figure 2(a) typical IEDFs are shown at the positions $z = 35$ cm and $z = 43$ cm, from upstream and downstream of the DL formation, respectively.

For these measurements, the probe was oriented with the aperture facing towards the source. Upstream a fitted single Gaussian distribution is centred at a plasma potential (V_p) of 55 V, taken at the maximum of the fitted Gaussian.

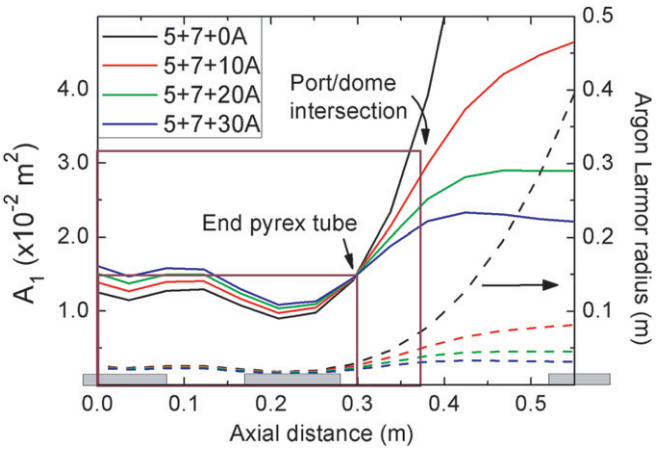

Figure 3. Area expansion of magnetic field lines, with reference area A_0 (cross-section of source) chosen at the entrance of the source tube, and shown for the same magnetic field configurations as in figure 1. Argon Larmor radii (dashed lines) are shown on the right-hand scale.

Downstream a double Gaussian fit with peaks at 36 V and 60 V is interpreted as plasma potential and beam potential (V_b), respectively. Note that the downstream V_b appears higher than the upstream V_p, which is somewhat counter-intuitive. This feature is however easily explained by inspecting the non-normalized IEDFs in figure 2(a). As ions at lower energies are more readily thermalized than those with larger energies the beam peak will be shifted upwards, but is still retained within the envelope of the upstream distribution which has much higher ion density. The plot in figure 2(b) shows a detailed axial scan of the potentials, and demonstrates that the beam is formed over a distance of less than 2 cm.

It appears more than 7 cm downstream from the end of the source tube and about 2 cm downstream of the intersection between the port and the dome of the chamber. This means that if the DL connected to the boundary between glass and metal at the base of the source tube, the curvature of the DL is almost circular. If the DL is connected to the port–dome intersection, implying formation by geometrically expanding plasma as found by Corr *et al* [22], the curvature radius is about 50 cm. On the other hand, a detailed radial mapping near the source tube and the port needs to be carried out in order to find the DL position also with respect to radial position.

We now introduce a current into the third coil at $z = 58$ cm. The purpose of this coil is to improve the downstream plasma confinement. Since it alters the plasma properties significantly, it is also necessary to understand its effect on the CFDL beam and plasma flow.

In figure 3 the area expansion of the flux lines from the edge of the source tube is shown for the same configurations as in figure 1, following the relation $A_0 B_0 = A(z)B(z)$, where A_0 and B_0 are the area and magnetic field at the edge of the tube, respectively. We consider electrons following the magnetic field lines from the source through the 7 cm long port 'neck' into the main chamber. At zero or low field contribution from the third coil, a portion of the electrons will be lost to the port walls directly along the field lines. From figure 3, it is observed that approximately 5 A is needed in the third coil to

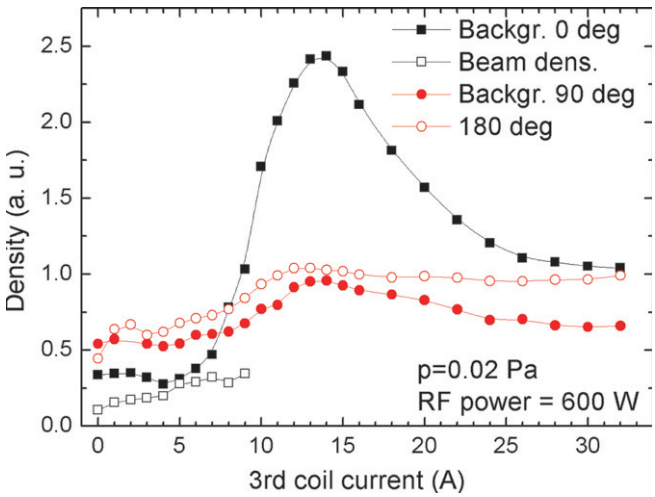

Figure 4. Beam and plasma background areas from fitted Gaussians (proportional to ion densities) plotted as a function of third coil current at the centre of the plasma column at $z = 51$ cm, and with RFEA pointing towards the source (black squares), and at 90° and 180° away from the source (filled and open red circles, respectively). Beam densities are shown as open squares.

prevent the flux lines at the edge of the source from entering the port walls. At 10 A all the field lines within the source cross-section are also contained within the cross-section (A_1) of the port–dome intersection. The Larmor radii of the ions are shown on the right-hand scale of figure 3. With no magnetic field contribution from the third coil, it increases from about 4 cm at the source entrance to nearly 10 cm at the port–dome intersection. At 10 A in the third coil it reduces to about 5 cm at the port–dome intersection.

The areas of the fitted Gaussians, proportional to the ion densities, are shown in figure 4. The background density as measured by the RFEA at 90° and 180° with respect to the source (filled and open circles, respectively), increases by nearly a factor of 2 as the magnetic field increases from 0 to 13 A in the third coil. The maximum at 13 A corresponds to an area A ($z = 37.3$ cm) less than A_1. With the probe facing the source, a beam is observed at lower magnetic fields. It can also be seen that when the beam is present, the sum of the beam and background densities at 0° is in agreement with the background density from the RFEA at 90° and 180°. The beam is observed until a sharp increase takes place in the background density measured at 0° as $A(z)$ decreases to values less than A_0. From the field when the beam disappears and a single Gaussian can be fitted to the IEDF, the density from the probe at 0° increases to a maximum nearly 2.5 times the maximum of the density from the measurement at 90°.

This might be attributed to an effect from a subsonic plasma flow set up when the beam disappears. At 180° rotation of the probe and lower magnetic fields, the apparent density is slightly higher or similar to that at 90°. It is thus feasible that an RFEA probe, when rotated at 0° and 180°, respectively, could behave similar to a Mach probe. Work is underway to investigate whether this discrepancy can be used as a measure of a bulk flow being set up in the plasma when the ion distribution becomes a single Gaussian.

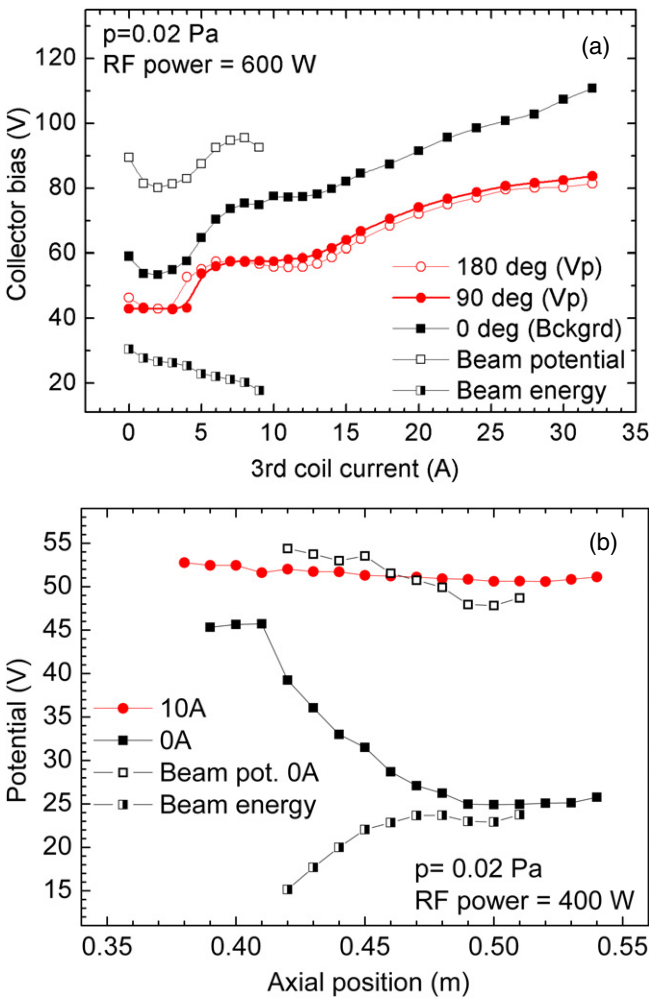

Figure 5. (*a*) Beam potentials (open squares), plasma potentials (filled squares and circles) and beam energies (half-filled squares) at $z = 51$ cm plotted as a function of third coil current, with the RFEA pointing towards the source (filled squares), and at 90° and 180° (filled and open circles) away from the source. In (*b*), plasma potentials, beam potentials and beam energies are plotted as a function of axial position for zero current in the third coil (squares). At 10 A, only plasma potentials (filled circles) are shown (beam was not found).

Figure 5(*a*) shows the development of beam and background potentials at the centre of the plasma column at $z = 51$ cm with increasing current in the third coil. The data were obtained with the radial RFEA facing the source, as well as 90° and 180° away from it. The beam energy is similar to the beam energies shown in the axial plots of figures 2 and 5(*b*). However, there is a discrepancy in absolute values of potential between the radial and axial probes. The reason for this is not yet fully understood. However, it should be noted that for the axial measurements, the probe head and aperture grid were floating with respect to ground, while for the radial measurement, both were grounded. The bulk plasma potential from the single Gaussian of the probe signal at 90° is almost exactly overlapping the potential measured by the RFEA at 180°. At low magnetic fields, first it is constant at about 40 V, followed by a sharp increase and a short plateau where the

ion density increases, as seen in figure 4. The background potential of the RFEA facing the source is significantly higher than V_p measured when it is turned away from the source, and the difference increases from about 10 V at low magnetic fields to about 30 V at the high B fields. This may be understood in terms of a wake field set up behind a negatively charged obstacle (the grounded RFEA) in a flowing plasma, analogous to what is predicted theoretically [23] for a test (dust) particle and numerically [24] for insulating dust grains in a supersonic non-magnetized plasma flow. The dimension of the RFEA is substantial (cross-sections of $\sim$2 cm), and hence the disturbance, particularly in the downstream direction, is significant. To calibrate the V_p measurements, emissive probe measurements have been carried out for low magnetic fields, and are underway also for higher magnetic fields.

The disappearance of the beam at higher currents than 8 A in the third coil is consistent with the axial measurements of potentials shown in figure 5(*b*). The beam-forming potential drop between the source and the downstream plasma has completely vanished at 10 A. The DL and beam formed at zero current are shown for comparison. Also in this case, the potential of the beam, formed at $z = 42$ cm, is higher than the upstream plasma potential, an effect discussed earlier for the data shown in figure 2(*b*).

In conclusion, the effect of a downstream magnetic field on the plasma parameters and DL beam formation in the new helicon source Njord has been studied. The plasma potential increases sharply as the area spanned by the magnetic field from the source tube decreases below A_0 at the port–dome intersection, and the plasma density increases due to improved magnetic confinement. The beam from the DL disappears as the plasma potential increases to approximately the same level as the source potential.

Acknowledgments

This work was funded by the Norwegian Research Council, Grant no 177570. The authors are grateful to I Strømmesen, T Roaldsen, K-A Willumstad and Y Eilertsen for their expert technical assistance, which was essential for the assembly and operation of this experiment. Christopher Watts, University of New Mexico, USA, most helpfully provided the Henry RF power amplifier for the plasma source.

References

[1] Marsch E *et al* 2008 *Astrophys. J.* **685** 1262
[2] Ganguli S B 1996 *Rev. Geophys.* **34** 311
[3] Ergun R E *et al* 2001 *Phys. Rev. Lett.* **87** 045003
[4] Mozer F S *et al* 1977 *Phys. Rev. Lett.* **38** 292
[5] Ergun R E *et al* 2004 *J. Geophys. Res.* A **109** A12220
[6] Raadu M A 1989 *Phys. Rep.* **178** 25
[7] Hershkowitz N 1985 *Space Sci. Rev.* **41** 351
[8] Block L P 1978 *Astrophys. Space Sci.* **55** 59
[9] Takahashi K *et al* 2007 *Phys. Plasmas* **14** 114503
[10] Ionita C, Dimitriu D G and Schrittwieser R W 2004 *Int. J. Mass Spectrom.* **233** 343
[11] Diebold D *et al* 1992 *IEEE Trans. Plasma Sci.* **20** 601
[12] Stenzel R L *et al* 2008 *Plasma Sources Sci. Technol.* **17** 035006
[13] Newman D L *et al* 2001 *Phys. Rev. Lett.* **87** 255001
[14] Sefkow A B and S A Cohen 2009 *Phys. Plasmas* **16** 053501
[15] Perkins F W and Y C Sun 1981 *Phys. Rev. Lett.* **46** 115
[16] Hairapetian G and R L Stenzel 1990 *Phys. Rev. Lett.* **65** 175
[17] Charles C and R W Boswell 2004 *Phys. Plasmas* **11** 1706
[18] Cohen S A *et al* 2003 *Phys. Plasmas* **10** 2593
[19] Charles C and R Boswell 2003 *Appl. Phys. Lett.* **82** 1356
[20] Charles C, Boswell R W and Porteous R K 1992 *J. Vac. Sci. Technol.* A **10** 398
[21] Byhring H S *et al* 2008 *Phys. Plasmas* **15** 102113
[22] Corr C S *et al* 2007 *Appl. Phys. Lett.* **91** 241501
[23] Lapenta G 2000 *Phys. Rev.* E **62** 1175
[24] Miloch W J *et al* 2009 *Phys. Plasmas* **16** 023703